

## Circle Deformation in Hacon's Sphere Eversion

Yongheng Zhang

Department of Mathematics and Statistics, Amherst College, MA, USA  
 yzhang@amherst.edu

### Abstract

This note records an approach to understand Derek Hacon's sphere eversion. In particular, Hacon's description and drawing of a regular homotopy of the outer cylinder was translated into an analytical expression, which is generated by deforming a circle along the temporal and a spatial dimension. The circle deformation is controlled by a two-parameter motion of finitely many points. This model was used in computer visualization and rapid prototyping.

### Introduction

Since Smale proved the existence of sphere eversion, many concrete descriptions of such processes have been found (e.g., [5]), although all are difficult to understand. In the 1970s, Derek Hacon discovered a particularly elegant eversion [2], which was not widely known until much later. In 2016, Polster explained Hacon's eversion in a Mathologer video [4], which had more than 250,000 views at the time of this writing.

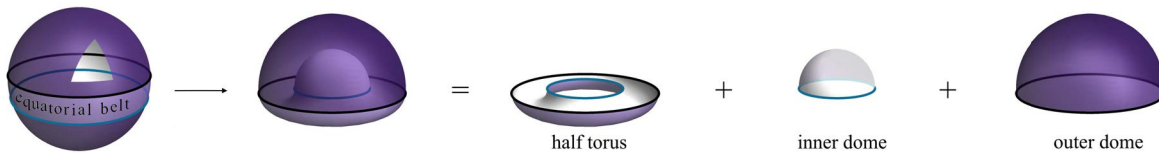


**Figure 1:** A triangle was cut off to show the inside; Derek Hacon's formula  $sphere = \frac{1}{2} \text{torus} + 2 \text{domes}$

In Hacon's eversion, the sphere is decomposed into three parts: the southern hemisphere, the northern hemisphere and an equatorial belt connecting the two. First, the southern hemisphere is pushed toward the northern hemisphere so that they become the inner dome and the outer dome while the equatorial region is morphed into half a torus (Figure 1). Then, as its two boundary circles stay on the plane  $z = 0$ , the half torus undergoes a deformation which eventually flips its two sides. At the same time, the inner and outer domes trade their locations. Lastly, the new inner dome (which was the northern hemisphere) is pushed downward. The original sphere now is turned inside out!

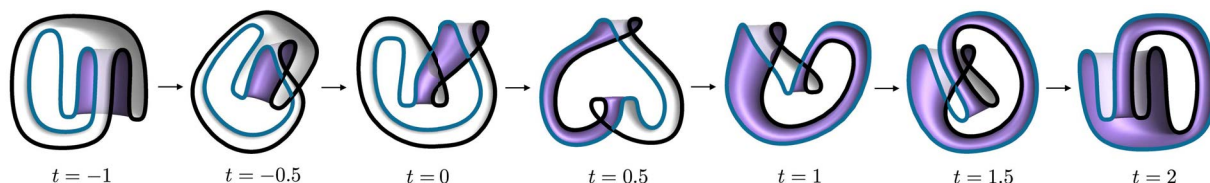


**Figure 2:** Hacon's half-torus eversion. The  $t$  values are for later reference.

The half-torus eversion is shown in Figure 2. These seven frames are renderings of the pictures on the first page of Hacon's note [2]. The beautiful video [1] by Chérítat animates a similar eversion, whose spatial mirror image is homotopic to that of Hacon. The inner dome and outer dome deformations follow those of

their base circles. As the base circle (in blue-gray) of the inner dome is always a simple closed curve, the inner dome can stay embedded (without self-intersections), and we can animate its motion in our mind. The base circle (in black) of the outer dome, however, crosses itself multiple times under the deformation. Thus, the motion of the outer dome, which is an immersed rather than an embedded surface most of the time, is more complicated. This note aims to explain some details of the deformation of the outer dome.

### Regular Homotopy of the Outer Cylinder

For each  $t \in [-1, 2]$  and  $z \in [0, 1]$ , I will construct an immersed planar circle  $C_t^z$ , which collectively give us an analytical two-parameter circle deformation, along the temporal dimension  $t$  and the spatial (elevation) dimension  $z$ . The seven base circles (in black) in Figure 2 are  $C_t^0$ , for  $t = -1, -0.5, 0, 0.5, 1, 1.5$ , and  $2$ . I will describe a way to interpolate among them to generate  $C_t^z$  for all  $t$ , and then deform them to generate  $C_t^z$  for all  $t$  and  $z$ , such that for each  $t$ ,  $C_t^1$  is an embedded circle. The immersed outer dome at each time instance  $t$  is the union of an immersed cylinder and an embedded roof, which meet along the simple closed curve  $C_t^1$  on the plane  $z = 1$ . The roof follows  $C_t^1$ , which doesn't have self-intersection, so we can simply picture the roof's movement in our head. For each  $t$ , stacking the intermediate curves in a deformation from  $C_t^0$  to  $C_t^1$  as  $z$  goes from 0 to 1 generates each immersed cylinder  $Cyl_t$ , which will be our focus.

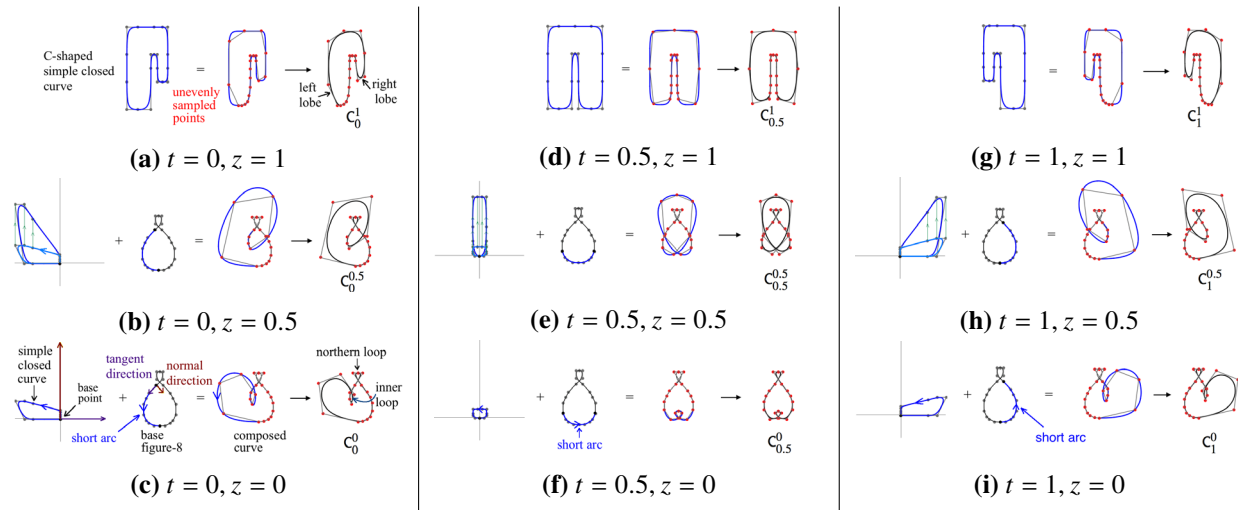


**Figure 3:** Deformation of the immersed circle (in black) is controlled by the motion of 20 points (in red).

In [2], Hacon described the deformation of  $C_t^z$  by indicating the movement of 4 points on each circle, which suggests that (cubic) B-splines could be used to generate analytical expressions (piecewise polynomials) for  $C_t^z$ , whose deformation are controlled by the motion of more, in our case 20, control points.

Let's start by focusing on frames 3 to 5 in Figure 2, during which the inner loop travels counterclockwise from west to east as  $t$  goes from 0 to 1. At the earlier stage of this research, I tried to model the loop motion by moving the 20 control points directly. However, I found it very challenging to produce a visually satisfying result. In any way, the control points need to make their moves in a coordinated manner. It would not be a good idea to move the control points individually in order to produce loop motion. Later, I adopted a technique which was inspired by Thurston's corrugation method [3] (Figure 3c,f,i). First, a base figure-8 curve (in gray) was generated using B-splines. Then a short arc (in blue) on it is identified and it moves counterclockwise from west to east as  $t$  goes from 0 to 1. Afterwards, a B-spline-generated simple closed curve, whose base point is the origin, is added to the blue short arc, after being point-wise rotated by the unit-tangent-unit-normal orthogonal frames of the blue short arc. In the corrugation method, multiple

figure-8 curves are added to a base curve. Here, a single simple closed curve is added to the base figure-8.

Now, the composed curve contains an inner loop. As we move the blue short arc, the inner loop also moves. We can also control the shape of the inner loop by moving the control points of the added simple closed curve, in this case, simply along individual straight lines (Figure 3b,e,h). As  $z$  changes from 0 to 0.5, the inner loop moves towards north and is enlarged. See the transition from Figure 3c,f,i to Figure 3b,e,h. Now, we can evenly choose 20 points in the domain of each composed parametrized curve, with points closest to the center of the northern loop modified to maintain  $C^1$  regularity. These 20 points in turn generate another curve, which is our  $C_t^z$ .

To see what happens for  $0.5 \leq z \leq 1$ , a C-shaped simple closed curve was first constructed using B-splines, whose left and right lobes trade their sizes as  $t$  goes from 0 to 1. Again, 20 points were chosen on each curve, this time unevenly to avoid singularity, but with modification for  $C^1$  regularity as well (Figure 3a,d,g). The 20 points for each  $C_t^{0.5}$  are moved to these 20 points along individual straight lines, so that they generate  $C_t^z$  for all  $z$  between 0.5 and 1 and all  $t$  between 0 and 1. As  $z$  changes from 0.5 to 1, the two lobes of each immersed circle are separated, so that for each  $t$ ,  $C_t^1$  is simple-closed. Overall, for  $0 \leq t \leq 1$  and  $0 \leq z \leq 1$ , the deformation of these 20 points gives us the deformation of  $C_t^z$ .

The above deformation corresponds to page 2–5 of Hacon's note [2].

To complete the process, a "space-time rotation" is needed, as shown in Figure 4, where the immersed circles along each diagonal line are the same, and so are the immersed circles in the two shaded triangles (in light gray). Thus,  $Cy1_t$  for  $-1 \leq t \leq 0$  and  $1 \leq t \leq 2$  are generated from  $Cy1_0$  and  $Cy1_1$ , respectively. This corresponds to the last two pages (6–7) of [2]. Also note that Figure 4 is symmetric about  $t = 0.5$ .

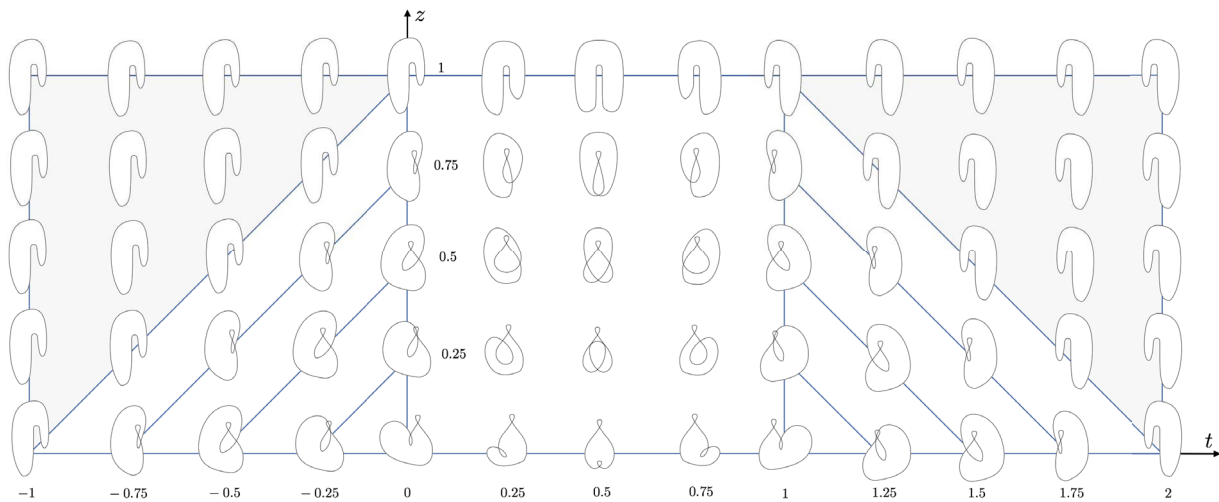


**Figure 4:** Immersed circle "field": Cross sections  $C_t^z$  of immersed cylinders on the parameter domain.

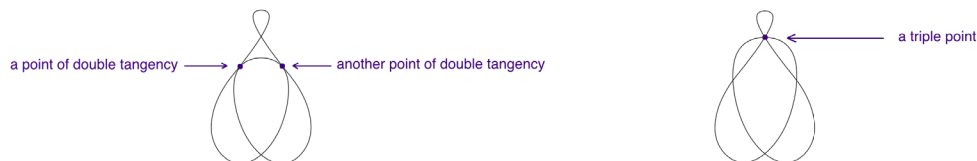


**Figure 5:** Cross sections  $C_t^z$  at  $t = 0.5, z \approx 0.252$  (left) and  $t = 0.5, z \approx 0.287$  (right).

Fix any  $t$  between 0 and 1, as  $z$  increases from 0 to 1,  $C_t^z$  has to pass through at least one triple point (where three different points on the immersed circle meet), and three points of double tangencies (where two different segments of the immersed circle are tangent to each other) (Figure 5). Indeed, all cross sections in columns

$t = 0, 0.25, 0.5, 0.75$  and  $1$  of Figure 4 passed through exactly one triple point. They passed through five points of double tangencies in the column  $t = 0.5$ , and three in the columns  $t = 0, 0.25, 0.75$  and  $1$ .

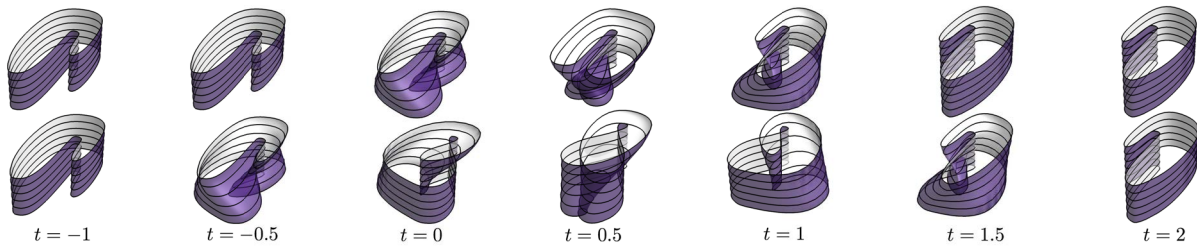


**Figure 6:** Immersed upper ( $0.5 \leq z \leq 1$ ) and lower ( $0 \leq z \leq 0.5$ ) cylinders corresponding to Figure 2.

Figure 6 shows computer generated pictures of the upper ( $0.5 \leq z \leq 1$ ) and lower ( $0 \leq z \leq 0.5$ ) cylinders at  $t = -1, -0.5, 0, 0.5, 1, 1.5$  and  $2$ . Care has been taken to ensure that each pair of half cylinders match smoothly. See also the 3D prints in Figure 7, which are hard to understand without some knowledge of their cross sections. In case the reader would like to play with some animations, or is interested in more technical details, a Mathematica notebook can be found on this paper's Bridges Archive webpage.

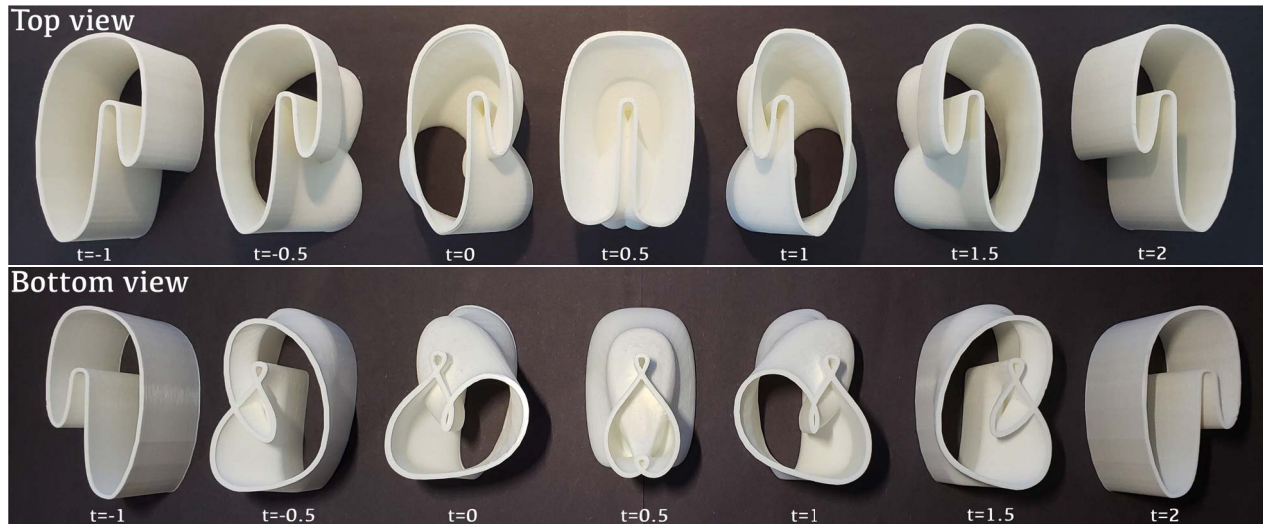


**Figure 7:** 3D prints of immersed outer cylinders corresponding to Figure 2.

### Acknowledgements

The author is grateful to the reviewers for their detailed comments, which improved the paper in many ways.

### References

- [1] A. Chéritat. <http://youtu.be/Cw4aTVi8ndQ>. November, 2016.
- [2] D. Hacon. <http://www.math.utah.edu/~hacon/sphereeversion.pdf>. Mid 1970s?
- [3] S. Levy and W. Thurston. *Making Waves – A Guide to the Ideas behind Outside In*. The Geometry Center, University of Minnesota, 1995. A K Peters/CRC Press, 2009.
- [4] B. Polster. <http://youtu.be/ixduANVe0gg>. November, 2016.
- [5] J. M. Sullivan. <http://torus.math.uiuc.edu/jms/Papers/isama/color/opt2.htm>. 1999.